



**HAL**  
open science

## The role of Arginine 38 in Horseradish Peroxidase enzyme revisited: A computational investigation

Simone Tatoli, Costantino Zazza, Nico Sanna, Amedeo Palma, Massimiliano Aschi

► **To cite this version:**

Simone Tatoli, Costantino Zazza, Nico Sanna, Amedeo Palma, Massimiliano Aschi. The role of Arginine 38 in Horseradish Peroxidase enzyme revisited: A computational investigation. *Biophysical Chemistry*, 2009, 141 (1), pp.87. 10.1016/j.bpc.2008.12.015 . hal-00531139

**HAL Id: hal-00531139**

**<https://hal.science/hal-00531139>**

Submitted on 2 Nov 2010

**HAL** is a multi-disciplinary open access archive for the deposit and dissemination of scientific research documents, whether they are published or not. The documents may come from teaching and research institutions in France or abroad, or from public or private research centers.

L'archive ouverte pluridisciplinaire **HAL**, est destinée au dépôt et à la diffusion de documents scientifiques de niveau recherche, publiés ou non, émanant des établissements d'enseignement et de recherche français ou étrangers, des laboratoires publics ou privés.

## Accepted Manuscript

The role of Arginine 38 in Horseradish Peroxidase enzyme revisited: A computational investigation

Simone Tatoli, Costantino Zazza, Nico Sanna, Amedeo Palma, Massimiliano Aschi

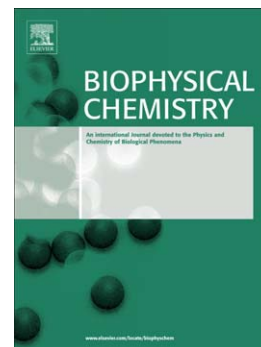
PII: S0301-4622(09)00003-9  
DOI: doi: [10.1016/j.bpc.2008.12.015](https://doi.org/10.1016/j.bpc.2008.12.015)  
Reference: BIOCHE 5214

To appear in: *Biophysical Chemistry*

Received date: 29 October 2008  
Revised date: 29 December 2008  
Accepted date: 30 December 2008

Please cite this article as: Simone Tatoli, Costantino Zazza, Nico Sanna, Amedeo Palma, Massimiliano Aschi, The role of Arginine 38 in Horseradish Peroxidase enzyme revisited: A computational investigation, *Biophysical Chemistry* (2009), doi: [10.1016/j.bpc.2008.12.015](https://doi.org/10.1016/j.bpc.2008.12.015)

This is a PDF file of an unedited manuscript that has been accepted for publication. As a service to our customers we are providing this early version of the manuscript. The manuscript will undergo copyediting, typesetting, and review of the resulting proof before it is published in its final form. Please note that during the production process errors may be discovered which could affect the content, and all legal disclaimers that apply to the journal pertain.



## The role of Arginine 38 in Horseradish Peroxidase enzyme revisited: a computational investigation

Simone Tatoli  
CASPUR,  
Via dei Tizii, 00185, Rome, Italy.  
Dipartimento di Chimica Università di Roma 'La Sapienza'  
P.le A. Moro 5, 00185, Rome, Italy.

Costantino Zazza  
CASPUR,  
Via dei Tizii, 00185, Rome, Italy.

Nico Sanna  
CASPUR,  
Via dei Tizii, 00185, Rome, Italy.

Amedeo Palma<sup>1</sup>  
Istituto per lo Studio dei Materiali Nanostrutturati,  
CNR-ISMN, via Salaria Km. 29.3, Sez. Montelibretti,  
Monterotondo S.(RM), Italy.

Massimiliano Aschi<sup>2</sup>  
Dipartimento di Chimica , Ingegneria Chimica e Materiali,,  
Università di L'Aquila, via Vetoio 67100, L'Aquila, Italy.

<sup>1</sup>Istituto per lo Studio dei Materiali Nanostrutturati, CNR-ISMN, via Salaria Km. 29.3, Sez. Montelibretti, Monterotondo S.(RM), Italy.  
E-mail address: [amedeo.palma@ismn.cnr.it](mailto:amedeo.palma@ismn.cnr.it)

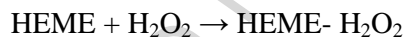
<sup>2</sup>Dipartimento di Chimica , Ingegneria Chimica e Materiali, Università di L'Aquila, via Vetoio 67100, L'Aquila, Italy.  
E-mail address: [aschi@caspur.it](mailto:aschi@caspur.it)

**ABSTRACT:** Molecular dynamics simulations on hydrogen peroxide complex with wild-type (WT) and Arg38Leu mutated (R38L) Horseradish Peroxidase (HRP) were carried out over nanoseconds timescale in water solution at 300 K. Comparison of the results provides interesting insights about the role of highly conserved Arg38 and His42 residues in the chemical features of HRP, underlying its biological activity which initiates with Compound0 (Cpd0). In the WT-HRP enzyme current molecular dynamics simulations show, for the first time, that Arg38 residue: *i*) prevents the entrance of water inside the reaction cavity, hence providing a hydrophobic reactive scenario, *ii*) it maintains the distance between His42 and heme-H<sub>2</sub>O<sub>2</sub> complex suitable for the occurrence of proton transfer reaction leading, thereafter, to heme-H<sub>2</sub>O<sub>2</sub> disruption according to Poulos-Kraut mechanism. On the other hand, R38L mutant can be considered as a "wet enzyme" where the presence of water solvent molecules in the heme reaction pocket, unfavoring the initial heme-H<sub>2</sub>O<sub>2</sub> complex formation, decreases the catalytic efficiency in agreement with experimental kinetics measurements. Furthermore, we note that Arg38Leu mutation pushes the His42 residue far from the heme-H<sub>2</sub>O<sub>2</sub> complex, making unlikely a direct proton transfer and suggesting that, in the mutant, a solvent water molecule could be involved in the first step of the Poulos-Kraut mechanism.

**Keywords:** Horseradish Peroxidase enzyme; R38L Mutant; Classical Molecular Dynamics simulations.

## INTRODUCTION

Among the heme peroxidases, horseradish peroxidase (HRP) is one of the most studied enzymes for its importance in modern enzymology. HRP, in fact, catalyses a variety of organic and inorganic reactions utilizing hydrogen peroxide ( $\text{H}_2\text{O}_2$ ) and, in so doing, also protects the cell against accumulation of dangerously reactive  $\text{H}_2\text{O}_2$  (1). The rather complex catalytic cycle begins with the formation of ferric resting form of the heme peroxidase, in which the fifth coordination position of the heme iron is occupied by a proximal histidine side chain and the sixth coordination position by an aquo-ligand. The initial step in the mechanism of action is the interaction of  $\text{H}_2\text{O}_2$  with the ferric resting state of heme peroxidase to form hydroperoxo-ferric complex (heme- $\text{H}_2\text{O}_2$ ) which converts to Compound 0 (Cpd0) and eventually yields, by means of heterolytic O-O bond cleavage, the active species, Compound I (CpdI), according to the following scheme:



All the intermediates appearing in the scheme reported above have been isolated and characterized, although the molecular details of the process is not yet fully understood.

A commonly accepted mechanism for peroxidases is that one proposed, already many years ago by Poulos-Kraut (2), which involves stepwise acid-base catalysis through the highly conserved His42 and Arg38 residues in the distal side. The above residues are supposed to play a relevant role (3). As a matter of fact, Cpd0, a ferric-hydroperoxide anion, has been shown both experimentally (4–9) and theoretically (10–15) to be formed via deprotonation of  $\text{H}_2\text{O}_2$  by His42 acting as a base. Subsequently, CpdI, a ferric-oxo radical cation, is obtained by heterolytic O-O bond breaking after back protonation from His42 to the distal OH group of Cpd0. This mechanism is hypothesized for neutral or high pH where the His42 is neutral and Arg38 is in its cationic form (16).

On the other hand, less understood is the role of the highly conserved (17) residue Arg38. Experimental evidences, derived by substituting Arginine with a neutral residue as Leucine

(Arg38Leu) (17) have suggested that Arg38 is involved in the cleavage of O-O bond and, most of all plays an important role in enhancing the efficiency of the binding of H<sub>2</sub>O<sub>2</sub> to heme, contributing to the hydrogen bonding network formation in the distal pocket. This effect, if compared to the one produced by His42 which definitely acts as a Brønsted base, may be roughly considered as indirect and is much more difficult to be rationalized.

Recent literature (18–20) has shown that, under native conditions, biomacromolecules should be considered as an ensemble of conformational states rather than as a single static picture, being subject to thermal fluctuations and conformational transitions which might play a key-role in fine tuning the biological activity. Similar conclusion was drawn in our previous paper (15), where it was found that after an exothermic and mechanically hindered proton transfer (from H<sub>2</sub>O<sub>2</sub> to His42), the reaction pocket at room temperature is in equilibrium between two conformations, differing essentially for the His42 position, and Cpd0 formation is therefore characterized by a large entropic contribution.

In the present study, as a continuation of our previous investigation on HRP reactivity (15), we use nanoseconds time-scale Molecular Dynamics (MD) simulations in order to shed some light on the role of Arg38 in HRP enzyme. Interestingly, by comparing simulations of aqueous H<sub>2</sub>O<sub>2</sub> complex of the wild type (hereafter labelled as HRP-H<sub>2</sub>O<sub>2</sub>) and Arg38Leu mutant (hereafter termed as R38L-H<sub>2</sub>O<sub>2</sub>, see Figure 1), we find that Arg38 function is not only limited, as usually thought, to stabilize Cpd0 and to favour CpdI formation by electrostatic effects, but also to control water accessibility with respect to the reaction pocket. Moreover, our theoretical/computational investigation indicates that upon point mutation the distal side of the heme reaction pocket undergoes a conformational transition which basically pushes the His42 side chain far from the peroxy-complex. This finding is important for two reasons: firstly, because it shows how enzyme dynamics and reactivity change as a consequence of a point mutation, secondly, because it re-opens the issue about the reaction mechanism leading to Cpd0 in R38L.

The paper is organized as follows: in the first part we report the computational details

regarding our classical MD simulations. Afterwards we describe the main results of our theoretical investigation on the HRP-H<sub>2</sub>O<sub>2</sub> and R38L-H<sub>2</sub>O<sub>2</sub> bio-molecular systems in two different subsections: structural and mechanical properties of the C-alpha of the two simulated systems; Local effects induced by Arg38Leu point mutation on the heme reaction pocket. Finally, we summarize the basic features of the HRP- H<sub>2</sub>O<sub>2</sub> and R38L-H<sub>2</sub>O<sub>2</sub> systems.

## METHODS

### Computational details

As previously described in our recent computational study on HRP reactivity, simulations were initiated using, as starting coordinates, HRP monomer extracted from the crystal structure of recombinant peroxidase (see Figure 2). In the first simulated system, HRP-H<sub>2</sub>O<sub>2</sub>, the protein framework was adopted throughout with H<sub>2</sub>O<sub>2</sub> occupying the sixth coordination of iron, see Figure 1. In the second simulated system, R38L-H<sub>2</sub>O<sub>2</sub>, we used exactly the same starting coordinates of the first simulation with Arginine in position 38 substituted with Leucine. Structural Ca<sup>2+</sup> ions were also included in the system because of their documented importance in maintaining the structural integrity of heme (21). The solutes (HRP-H<sub>2</sub>O<sub>2</sub> and R38L-H<sub>2</sub>O<sub>2</sub>) were put at the centre of a rectangular box (74.5x87.2x69.7 Å<sup>3</sup>) filled with Single Point Charge (22) (SPC) water molecules at a density of 1000 kg/m<sup>3</sup> (13371 SPC water molecules). A standard protocol was adopted for initiating the simulations: the charges of the protein have been adjusted according to Gromacs tool (pdb2gmx) (23) with Gromos force field (24) assuming pH=7. As far as the other salts were concerned we just added the proper number of counterions (one Cl<sup>-</sup>) to ensure the overall electrical neutrality of the system. Following a geometry optimization of the solute, the system was gradually heated from 50 K to 300 K using short (20 ps) MD simulations.

The trajectories were then propagated for 20 ns in a NVT ensemble using an integration step of 2.0 fs with the rototranslational constrain (25) applied to the solute. It is worth noting that these simulations are, at least to our knowledge, the longest ever performed on such system.

The temperature was kept constant by the isokinetic temperature coupling (26) and all bond lengths were constrained using LINCS algorithm (27). Long range electrostatics was computed by the Particle Mesh Ewald method (28) with 34 wave vectors in each dimension and a 4th order cubic interpolation. Gromos force field (24) parameters were adopted for the protein, for heme-H<sub>2</sub>O<sub>2</sub> the point charges were recalculated by standard fitting procedure (29) using a Density Functional Theory (30) calculations with the Becke's three parameters exchange and the Lee, Yang and Parr correlation functionals (B3LYP)(31, 32) with the following atomic basis sets: (i) for iron we used LANL2DZ effective core potential for the inner electrons (33) and a Double Zeta gaussian basis set of (5S,5P,5D)/[3S,3P,2D] quality for valence electrons (34); (ii) for nitrogen and oxygen we used a standard 6-311G(d) (35) gaussian basis set; (iii) for carbon and hydrogen 3-21G gaussian basis set was adopted.

Essential Dynamics (ED) analysis (36) of the trajectories of atomic coordinates was used to characterize conformational changes. This method consists of building the covariance matrix of the atomic positional fluctuations obtained from MD simulations. After its diagonalization, an orthonormal set of vectors (eigenvectors) defines a new set of generalized coordinates along which the fluctuations occur. The eigenvectors with the largest eigenvalues allow to define the essential subspace where to search for the relevant conformational transitions.

Finally, the distance R between the nitrogen atom of His42 and the proximal H<sub>2</sub>O<sub>2</sub> hydrogen has been monitored along both simulations and the related probability densities has been calculated. All the simulations were carried out using the Gromacs software (23); Quantum chemical calculations were performed using the Gaussian 03 package (37).



## RESULTS

### Structural and mechanical properties of HRP-H<sub>2</sub>O<sub>2</sub> and R38L-H<sub>2</sub>O<sub>2</sub>.

We first analyzed the global, structural and mechanical, effects induced by the Arg38Leu point mutation on the protein framework. HRP structure (see Figure 2) is dominated by alpha-helices with only two short anti-parallel beta-strands. This important feature, as already outlined in previous studies, (15, 38), justifies the rather low deviation of simulated aqueous HRP-H<sub>2</sub>O<sub>2</sub> from the crystal structure (root mean square deviation of 1.6 Å with a standard deviation of 0.4 Å). At the same time, and not surprisingly, the mutation in position 38 does not produce relevant structural alterations of R38L-H<sub>2</sub>O<sub>2</sub> with respect to the HRP-H<sub>2</sub>O<sub>2</sub>: we obtained a root mean square deviation of 1.7 Å with a standard deviation of 0.2 Å. In order to better compare the two systems we carried out ED analysis on the wild-type and mutant protein C-alpha, respectively.

In Figure 3 we report the projection of the two trajectories onto the plane defined by the first two eigenvectors (largest eigenvalues) obtained from the diagonalization of HRP-H<sub>2</sub>O<sub>2</sub> C-alpha covariance matrix, while the traces of the covariance matrices resulted equal to 334 Å<sup>2</sup> for HRP-H<sub>2</sub>O<sub>2</sub> and 267 Å<sup>2</sup> for R38L-H<sub>2</sub>O<sub>2</sub>. These results suggest that at room temperature HRP-H<sub>2</sub>O<sub>2</sub> and R38L-H<sub>2</sub>O<sub>2</sub> can be considered as rather rigid systems. At the same time, the Arg38Leu mutation induces a sharp reduction of the internal flexibility of the C-alpha (lower trace) without dramatically altering the character of the fluctuation (good superposition of the spots in Figure 3). A better comprehension of the overall effects produced by the mutation can be derived by the analysis of the atomic component for the first two ED eigenvectors.

To this end, we report in Figure 4 the atom composition of the first two ED eigenvectors. In order to assess the actual differences between the internal fluctuations of the two systems we also calculated the average difference, and the related maximum error, between WT-HRP and R38L eigenvector evaluated within two halves of the related trajectories. This analysis was carried out both for the first and the second eigenvector, see Figure 5.

Inspection of Figure 4 indicates that, as already suggested by the results reported in Figure 3, Arg38Leu mutation produces a relatively small variation in the internal fluctuation. The only remarkable differences, emerged upon mutation, concern the region close to the prosthetic centre, formed by Helix 21-34, Loop223-228 and Helix 87-94 (upper and lower right side of the heme indicated in blue in Figure 4) which turns out to slightly increase its fluctuation and the opposite side of HRP (indicated in yellow in the same Figure) which becomes more rigid upon mutation. Analysis of the maximum error reported in Figure 5 also points out that the above differences, although small, may be considered as significant within the simulated ensemble although some of the calculated errors result rather large indicating that more quantitative conclusions, out of the aim of the present study, would require much longer simulations.

#### **Local effects induced by Arg38Leu point mutation**

Let's now consider in details the local effects induced by mutation; in particular, comparing the flexibility of the key residues and the prosthetic centre forming the reaction pocket (schematically shown in Figure 1) before and after the point mutation. Comparison of the reaction pocket root mean square fluctuations (RMSF), reported in Figure 6 indicates that Arg38Leu mutation essentially produces an increase of His42 local fluctuation with respect to the other residues of the reaction pocket. It is also worth emphasizing the strong increase in the fluctuation pattern shown by Leu38 with respect the native Arg38.

In strict relationship with the previous analysis, we evaluated the probability distribution of the distance between the nitrogen atom of the His42 residue and the proximal proton of H<sub>2</sub>O<sub>2</sub> from MD simulations for HRP-H<sub>2</sub>O<sub>2</sub> and R38L-H<sub>2</sub>O<sub>2</sub>. Curves in Figure 7, explain the crucial, albeit indirect, role of Arg38 in the formation of Cpd0. The substitution of Arg38 removes the His42 from the acidic proton (right panel in Figure 7), thus suppressing the protonation of the latter by the heme-H<sub>2</sub>O<sub>2</sub> and preventing the overall process to occur. However, a further important effect has emerged from our MD simulations. In this respect, in Figure 8 we report the probability density for

a water molecule to occupy a position within a sphere of radius  $R$ , centred on the heme iron atom. The difference in the statistical distribution indicates a clear rearrangement of the water molecules for  $R$  ranging from 2-8 Å, upon point mutation. According to this finding and in agreement with experimental observations (38), the heme reaction pocket of the HRP-H<sub>2</sub>O<sub>2</sub> system shows a highly hydrophobic character, with zero normalized probability of finding a solvent molecule into the distal side (that is,  $R$  shorter than 4 Å) equal to zero. This is not the case with the R38L mutant where a complex diffusive process, driven by thermal fluctuations, is responsible for the transport of water molecules in the distal side of the pocket. Consequently, looking at the results reported in Figure 8, it is very interesting to observe that the Arg38Leu point mutation, removing the Arg38 which acts as a sort of gate (15), allows the entrance of water molecules in the reaction pocket. This effect may be explained by the above mentioned motions of the residues surrounding the reaction pocket (see Figure 6) as well as by the high flexibility of the Leucine side chain (see Figure 7) which opens the structural gate to water entrance as shown in Figure 9. Obviously, the increase of water concentration in the vicinity of heme-H<sub>2</sub>O<sub>2</sub> complex thermodynamically favours the formation of heme-H<sub>2</sub>O species. Our findings nicely support the experimental evidences about the reduced efficiency of H<sub>2</sub>O<sub>2</sub> to bind to iron upon mutation (17) and clearly shows that Arg38 works as a shelter which prevents the entrance of water molecules inside the heme reaction pocket. This effect of Arg38Leu mutation, restates the role of the Arg38 in wild-type HRP protein and hence, in the description of Cpd0 formation mechanism, reposes the decades old puzzle regarding the protonation and subsequent deprotonation of His42 residue.

In analogy with recent data published in literature (14), as a final step in our theoretical and computational investigation, we also evaluated the hydrogen-bonding interactions, at 300K, between distal SPC water molecules and the oxygen atom within the carbonyl group of the Pro139 residue (suitable as hydrogen bonding donor atom). The results of this analysis, reported in Figure 10, indicate that under the simulated conditions, a distal water molecule is coordinated to Pro139 by means of electrostatic interactions (see for example the right panel in Figure 9). From a statistical

point of view, it is worth to note that the most recurring value of the [(SPC)HOH... O=C(Pro139)] distance falls at about 1.7 Å. The same trend has been observed considering the proximal hydrogen of the H<sub>2</sub>O<sub>2</sub> as possible hydrogen bonding donor atom (i.e., [H<sub>2</sub>O... H(proximal)OOH] interatomic distance).

This means that, in our simulation conditions for R38L, Pro139, H<sub>2</sub>O<sub>2</sub> and one shared distal water molecule can provide a strongly cooperative hydrogen bonding network. Therefore, our classical MD simulations suggest that the recently proposed reaction mechanism in HRP enzyme, involving a water molecule as a proton vehicle catalyzing the formation of the Cpd0 intermediate (14) should be more appropriate for the R38L mutant rather than for the WT-HRP.

## CONCLUSIONS

Nanoseconds time-scale MD simulations at room temperature unequivocally show that the WT-HRP enzyme has a highly hydrophobic reaction pocket and this finding is exact in line with experiments(38); A critical analysis of the classical sampling supports the basic idea that such a result is essentially due to the formation of a strong hydrogen bonding glue between Arg38 side chain and peroxy-complex. This electrostatic interaction is not negligible, as it reinforces the presence of a persistent mechanical barrier given by the Arg38 position itself, which is able to prevent the water solvent molecules access into peroxy-complex cavity. It is also interesting to note that, the largely conserved Arg38 residue plays the biological role of protecting the formation of heme-H<sub>2</sub>O<sub>2</sub> complex and, therefore, it is crucial for the mechanism of formation of the CpdI in HRP, acting as a sort of "biological safety lock" driven by electrostatic interactions. So, present investigation does not support the involvement of a solvent water molecule in the proton transfer process which takes place in the first step of the Poulos-Kraut mechanism (2), albeit high energy barriers are found for such a reaction using state of the art calculations (14).

On the contrary, the R38L mutant, where the Arg38 residue is replaced by Leu, can be

characterized as a "wet" enzyme. More precisely, our data show that the point mutation might play an indirect and subtle key role in fine tuning the biological activity of the HRP enzyme. We show that the observed (17) and significant decrease in activity of the R38L mutant could be related also to the following findings: the Arg38Leu point mutation has the effect of exposing the reaction centre to water solvent molecules and, at the same time, increases the distance between the heme-  $H_2O_2$  and His42 making unlikely "a straight" proton transfer from peroxi-complex to distal histidine side chain. Moreover, in the R38L MD simulation, we observe the presence of a water molecule bridging Pro139 and  $H_2O_2$ . Thus let us suppose that, in this mutant, a solvent water molecule might act as an amphoteric shuttle for the the proton transfer during Cpd0 formation.

Our results further (20) indicate that the subtle and unexpected effects of a point mutation may be evidenced, at atomistic level, only explicitly taking into account fluctuations of the overall system including solvent. Moreover, investigations on spin curve crossing (doublet and quartet state) may be necessary to determine the "detailed" reaction mechanism in Cpd0 and CpdI formation in HRP.

#### **ACKNOWLEDGEMENTS**

We would like to thank Dr. A. Amadei (University of Tor Vergata, Rome) and Prof. S. Shaik (Hebrew University, Jerusalem) for interesting discussions. We are indebted to Dr. G. Chillemi (Caspur, Rome) for critically reading the manuscript. CNR (curiosity driven project N. 677) is gratefully acknowledged for financial support; Computational resources were provided by Caspur (Rome).

**REFERENCES**

- (1) T.L. Poulos. Peroxidases and Cytochrome P450 In The Porphyrin Handbook (Kadish K.M., Smith K.M., Guilard R., New York, 2000).
- (2) T.L. Poulos and J. Kraut, The stereochemistry of peroxidase catalys, *J. Biol. Chem* 255 (1980) 8199–8205.
- (3) M. Gajhede, D.J. Schuller, A. Henricksen, A.T. Smith and T.L. Poulos TL, Crystal structure of horseradish peroxidase C at 2.15 resolution, *Nat. Struct. Biol.* 4 (1997) 1032–1997.
- (4) H.K. Baek and H.E. Van Wart, Elementary steps in the formation of horseradish peroxidase compound I: direct observation of compound 0, a new intermediate with a hyperporphyrin spectrum, *Biochemistry* 28 (1989) 5714–5719.
- (5) H.K. Baek, H.E. Van Wart, Elementary steps in the reaction of horseradish peroxidase with several peroxides: kinetics and thermodynamics of formation of compound 0 and compound I, *J. Am. Chem. Soc.* 114(2) (1992) 718–725.
- (6) P. Douzou. In *Oxidases and Related Redox Systems*, Vol 1. (T. E. King, H. S. Mason, M. Morrison, editors. University Park Press, Baltimore, 1973).
- (7) I.G. Denisov, T.M. Makris and S.G. Sligar, Formation and Decay of Hydroperoxo-Ferric Heme complex in Horseradish Peroxidase Studied by Cryoradiolysis, *J. Biol. Chem.* 277 (2002) 42706–

42710.

(8) P. Jones and H.B. Dunford, The mechanism of Compound I formation revisited, *Journal of Inorganic Biochemistry* 99 (2005) 2292–2298.

(9) J.N. Rodrigues-Lopez, M.A. Gilabert, J. Tudela, R.N.F. Thorneley and F. Garcia-Canovas, Reactivity of Horseradish Peroxidase Compound II toward Substrates: Kinetic Evidence for a Two-Step Mechanism, *Biochemistry* 39 (2000) 13201–13209.

(10) G.H. Loew and M. Dupuis, Structure of a Model Transient Peroxide Intermediate of Peroxidases by ab Initio Methods, *J. Am. Chem. Soc.* 102 (1996) 10584–10587.

(11) D.E. Woon and G.H. Loew, An ab Initio Model System Investigation of the Proposed Mechanism for Activation of Peroxidases: Cooperative Catalytic Contributions from the Ion and Microsolvent Water, *J. Phys. Chem.* 102 (1998) 10380–10384.

(12) M. Wirstam, M.R.A. Blomberg and P.E.M. Siegbahn, Reaction Mechanism of Compound I Formation in Heme Peroxidases: A Density Functional Theory Study, *J. Am. Chem. Soc.* 121 (1999) 10178–10185.

(13) C. Zazza, M. Aschi and A. Palma, On the formation of Horseradish Peroxidase Compound I at high pH: New insights from ab initio molecular dynamics, *Chem. Phys. Lett.* 428 (2006) 152–156.

(14) E. Derat, S. Shaik, C. Rovira, P. Vidossich and M. Alfonso-Prieto, Effect of a Water Molecule on the Mechanism of Formation of Compound 0 in Horseradish Peroxidase, *J. Am. Chem. Soc.* (Communication) 129 (2007) 6346–6347.

- (15) C. Zazza, A. Amadei, A. Palma, N. Sanna, S. Tatoli and M. Aschi, Theoretical modelling of enzyme reactions: the thermodynamics of formation of compound 0 in horseradish peroxidase, *J. Phys. Chem. B.* 112 (2008) 3184–3192.
- (16) M. Filizola and G.H. Loew. Role of Protein Environment in Horseradish Peroxidase Compound I Formation: Molecular Dynamics Simulations of Horseradish Peroxidase-HOOH Complex, *J. Am. Chem. Soc.* 122(1) (2000) 18–25.
- (17) J.N. Rodriguez-Lopez, A.T. Smith and R.N.F. Thorneley, Role of Arginine 38 in Horseradish Peroxidase, *J. Biol. Chem.* 271(19) (1996) 4023–4030.
- (18) R. Spezia, M. Aschi, A. Di Nola, M. Di Valentin, D. Carbonera and A. Amadei, The effect of protein conformational flexibility on the electronic properties of a chromophore, *Biophys. J.* 84 (2003) 2805–2813.
- (19) A. Lodola, M. Mor, J. Zurek, G. Tarzia, D. Piomelli, J.N. Harvey and A.J. Mulholland, Conformational Effects in Enzyme Catalysis: Reaction via a High Energy Conformation in Fatty Acid Amide Hydrolase, *Biophys. J.* 92 (2007) L20–22L.
- (20) A. Amadei, M. D'Alessandro, M. Paci, A. Di Nola and M. Aschi, On the Effect of a Point Mutation on the Reactivity of CuZn Superoxide Dismutase: A Theoretical Study, *J. Phys. Chem. B* 110(14) (2006) 7538–7544.
- (21) M. Laberge, Q. Huang, R. Schweitzer-Stenner and J. Fidy, The endogeneous calcium ions of HRP C are required to maintain the functional nonplanarity of heme, *Biophys. J.* 84 (2003) 2542-



2552.

(22) H.J.C. Berendsen, J.P.M. Postma, W.F.V. Gunsteren and J. Hermans, Interaction models for water in relation to protein hydration. In *Intermolecular Forces*. (B. Pullman, Editor D. Reidel Publishing Company, Dordrecht 1981).

(23) D. Van der Spoel, A.R. Van Buren, E. Apol, P.J. Meulenhof, D.P. Tieleman, A.L.T.M. Sijbers, R. Van Drunen and H.J.C. Berendsen, In *Gromacs User Manual* version 1.3. (1996)

(24) W.F. Van Gunsteren, S.R. Billeter, A.A. Eising, P.H. Hunenberger, P. Kruger, A.E. Mark, V.R.P. Scott and I.G. Tironi IG, *Biomolecular simulation: The GROMOS96 manual and user guide*. (Hochschulverlag AG an der ETH, Zurich, 1996)

(25) A. Amadei, G. Chillemi, M. Ceruso, A. Grottesi and A. Di Nola, Molecular dynamics simulations with constrained roto-translational motions: theoretical basis and statistical mechanical consistency, *J.Chem. Phys.* 112 (2000) 9–23.

(26) H.J.C. Berendsen, J.P.M. Postma, W.F. Van Gunsteren and A. Di Nola, Molecular Dynamics with coupling to an external bath, *J. Chem. Phys.* 81 (1984) 3684–3690.

(27) B. Hess, H. Bekker, H.J.C. Berendsen and J.G.E.M. Frajje, LINCS: a linear constraint solver for molecular simulations, *J. Comput. Chem.* 18 (1997) 1463–1472.

(28) T.A. Darden, D.M. York and L.G. Pedersen, Particle mesh Ewald: method for Ewald sums in large systems, *J. Chem. Phys.* 98 (1993) 10089–10092.

- (29) C.M. Breneman and K.B. Wiberg, Determining atom-centered monopoles from molecular electrostatic potentials, *J. Comp. Chem.* 11 (1990) 361–367.
- (30) R.G. Parr and W. Yang, *Density functional theory of atoms and molecules.* (Oxford University Press, New York, 1999).
- (31) P.J. Hay and W.R. Wadt, Ab initio effective core potentials for molecular calculations. Potentials for K to Au including the outermost core orbitals, *J. Chem. Phys.* 82 (1985) 299–310.
- (32) C. Lee, W. Yang and R.G. Parr, Development of the ColleSalvetti correlation-energy formula into a functional of the electron density, *Phys. Rev. B* 37 (1988) 785–789.
- (33) A.D. Becke, Density-functional thermochemistry. III. The role of exact exchange, *J. Chem. Phys.* 98 (1993) 5648–5652.
- (34) T.H. Dunning Jr., Gaussian Basis Functions for Use in Molecular Calculations. I. Contraction of (9s5p) Atomic Basis Sets for the First-Row Atoms, *J. Chem. Phys.* 53 (1970) 2823–2833.
- (35) R. Krishnan, J.S. Binkley, R. Seeger and J.A. Pople, Self-consistent molecular orbital methods. A basis set for correlated wave functions, *J. Chem. Phys.* 72 (1980) 650–654.
- (36) A. Amadei, A.B.M. Linssen and H.J.C. Berendsen HJC, Essential dynamics of proteins. *Proteins: Struct., Funct. and Gen.* 17 (1993) 412–425.
- (37) M. J. Frisch, G. W. Trucks, H. B. Schlegel, G. E. Scuseria, M. A. Robb, J. R. Cheeseman, J. A.

Montgomery, Jr., T. Vreven, K. N. Kudin, J. C. Burant, J. M. Millam, S. S. Iyengar, J. Tomasi, V. Barone, B. Mennucci, M. Cossi, G. Scalmani, N. Rega, G. A. Petersson, H. Nakatsuji, M. Hada, M. Ehara, K. Toyota, R. Fukuda, J. Hasegawa, M. Ishida, T. Nakajima, Y. Honda, O. Kitao, H. Nakai, M. Klene, X. Li, J. E. Knox, H. P. Hratchian, J. B. Cross, V. Bakken, C. Adamo, J. Jaramillo, R. Gomperts, R. E. Stratmann, O. Yazyev, A. J. Austin, R. Cammi, C. Pomelli, J. W. Ochterski, P. Y. Ayala, K. Morokuma, G. A. Voth, P. Salvador, J. J. Dannenberg, V. G. Zakrzewski, S. Dapprich, A. D. Daniels, M. C. Strain, O. Farkas, D. K. Malick, A. D. Rabuck, K. Raghavachari, J. B. Foresman, J. V. Ortiz, Q. Cui, A. G. Baboul, S. Clifford, J. Cioslowski, B. B. Stefanov, G. Liu, A. Liashenko, P. Piskorz, I. Komaromi, R. L. Martin, D. J. Fox, T. Keith, M. A. Al-Laham, C. Y. Peng, A. Nanayakkara, M. Challacombe, P. M. W. Gill, B. Johnson, W. Chen, M. W. Wong, C. Gonzalez, and J. A. Pople, Gaussian 03, Revision C.02. Gaussian, Inc., Wallingford, CT, 2004.

(38) N. Mogharrab, H. Ghourchian and M. Amininasab, Structural Stabilization and Functional Improvement of Horseradish Peroxidase upon Modification of accessible lysines: Experiments and Simulation, *Biophys. J.* 92 (2007) 192–1203.

#### **FIGURE CAPTION**

Figure 1 : Left Panel: Schematic view of the HRP reaction pocket showing the relative positions of heme-H<sub>2</sub>O<sub>2</sub> complex, Arg38, His42, Pro139 and His170 residues. Right Panel: Same schematic view but for R38L mutant where the Arg38 amino acid residue is replaced by Leucine.

Figure 2: Pictorial view of Horseradish Peroxidase (HRP) enzyme. PDB code = 1ATJ.

Figure 3: Projection of the two trajectories onto the plane defined by the first and second eigenvector obtained from the HRP-H<sub>2</sub>O<sub>2</sub> (C-alpha) covariance matrix diagonalization.

Figure 4: Atom composition of the first (upper panel) and second eigenvector of the C-alpha covariance matrix of WT (black) and R38L (red) HRP. In the right-side panel we have evidenced the heme (red), the residue 38 (green). The regions undergoing a sharp increase of the (blue) or decrease (orange) of the fluctuation upon Arg38Leu point mutation are also shown.

Figure 5: WT-HRP and R38L average differences of the atomic composition of the first (red line in Panel A) and second (red line in Panel B) eigenvector with the related maximum error (black bars) calculated as semi-dispersion.

Figure 6: Root mean square (RMS) fluctuations of heme,  $H_2O_2$  and the residues occupying the reaction pocket.

Figure 7: Left panel: Probability distribution of the distance between the nitrogen atom of the His42 and the proximal proton of  $H_2O_2$  for HRP- $H_2O_2$  (solid line) and R38L- $H_2O_2$  mutant (dashed line). Right panel: Comparison of the most probable configurations (HRP- $H_2O_2$  in gray and R38L- $H_2O_2$  in dark-gray) obtained by using a least-squares fitting (mass weighted) procedure.

Figure 8: Normalized probability density for the presence of water molecules within a sphere of radius  $R$  centred on the heme iron atom. HRP- $H_2O_2$  (solid line), R38L- $H_2O_2$  (dashed line).  $R$  values shorter than 4 Å define volumes inside the distal heme pocket.

Figure 9: Left panel: Schematic view of the highly-hydrophobic reaction pocket of the WT-HRP enzyme during classical MD sampling at room temperature. Water molecules were only found outside the heme- $H_2O_2$  cavity(14). Right Panel: Same schematic view but for the R38L- $H_2O_2$  active site; water molecules found inside the distal heme pocket are shown.

Figure 10: Normalized probability density (see text) as a function of the[(SPC water molecule)

HOH ... O=C(Pro139)] interatomic distance obtained by R38L-H<sub>2</sub>O<sub>2</sub> classical trajectory at 300K.

ACCEPTED MANUSCRIPT

Fig 1

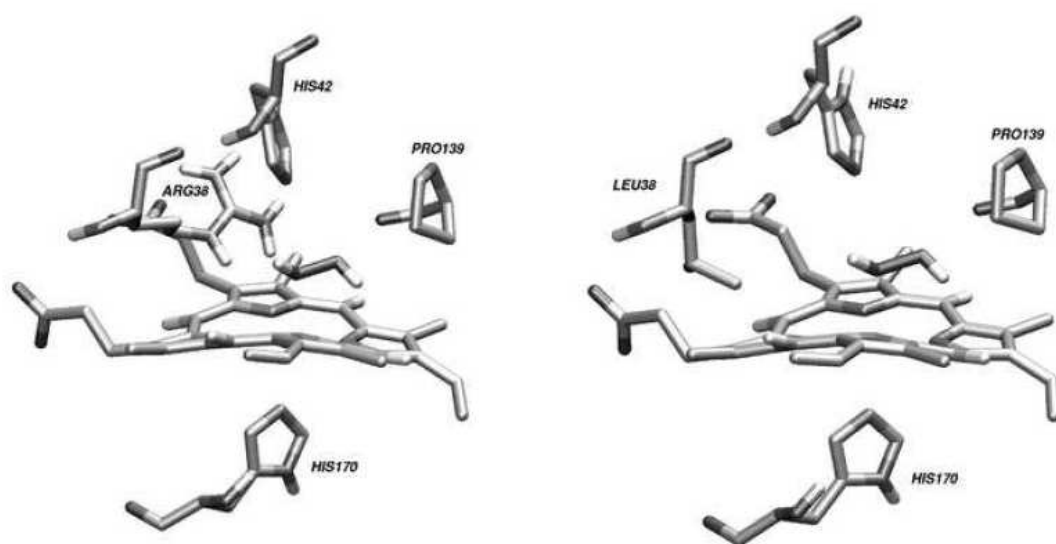


Fig 2

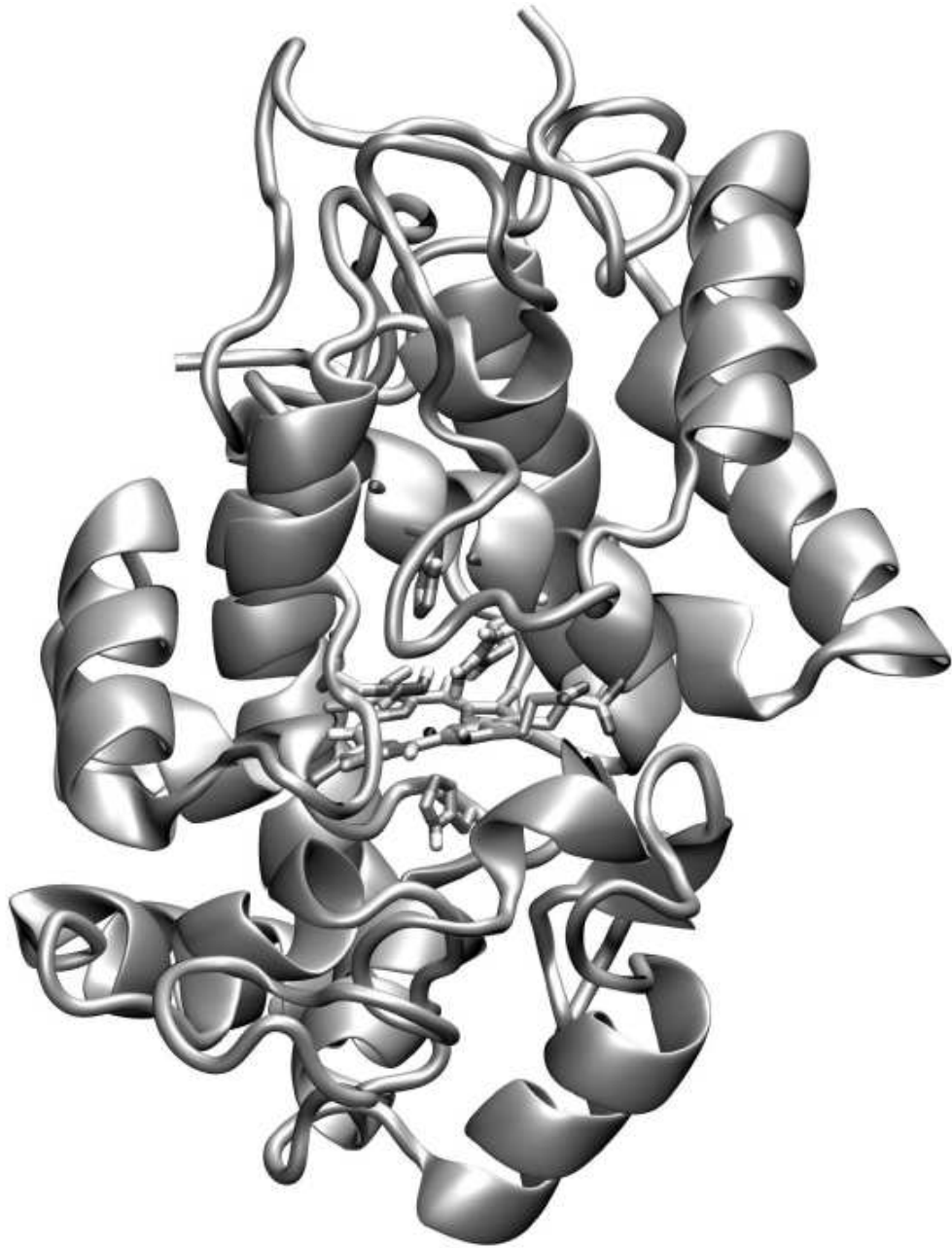


Fig 3

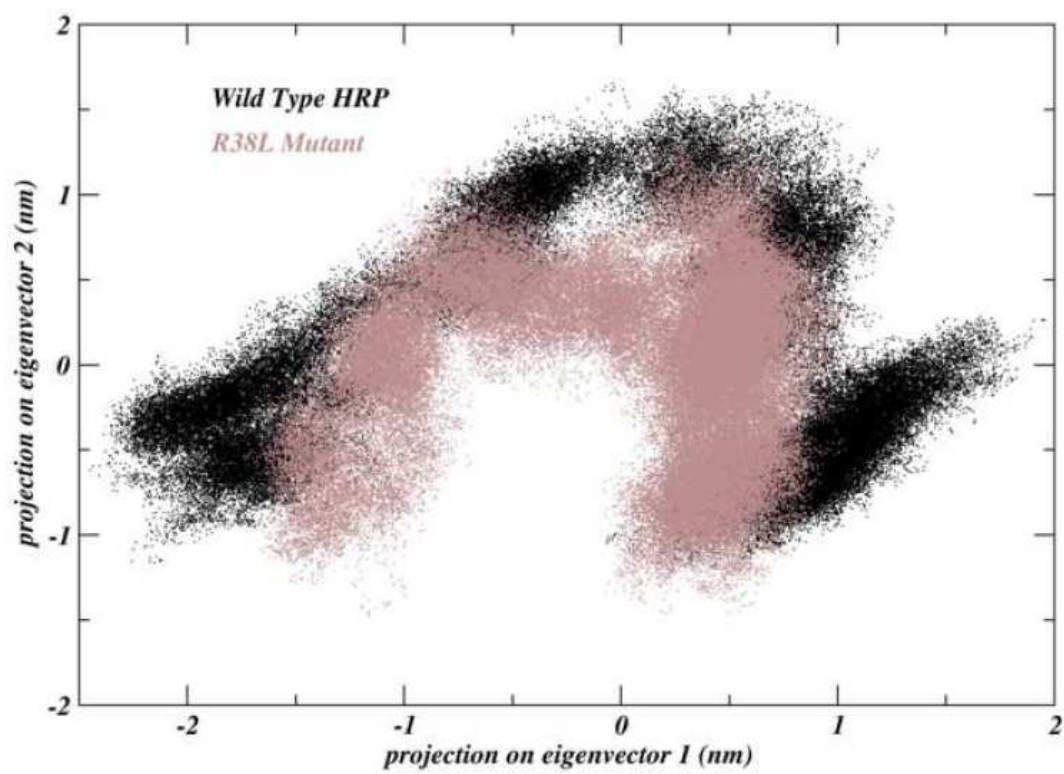
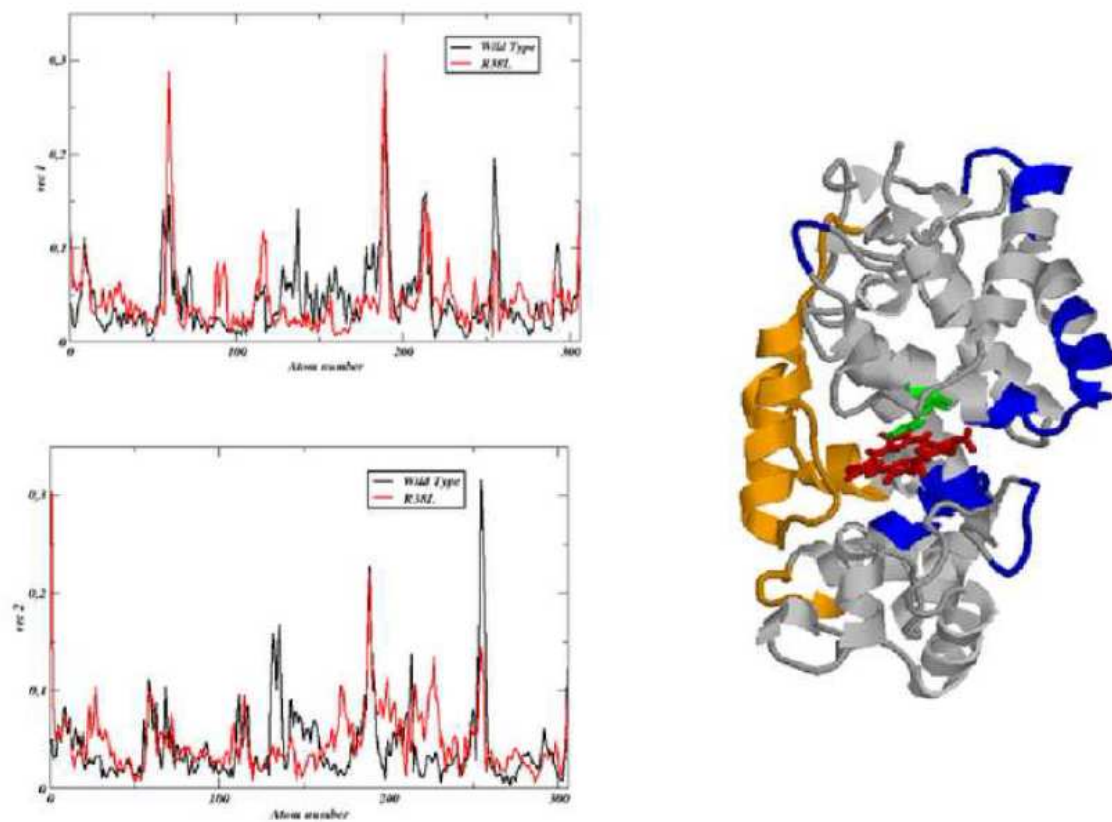




Fig 4



ACCEPTED

Fig 5

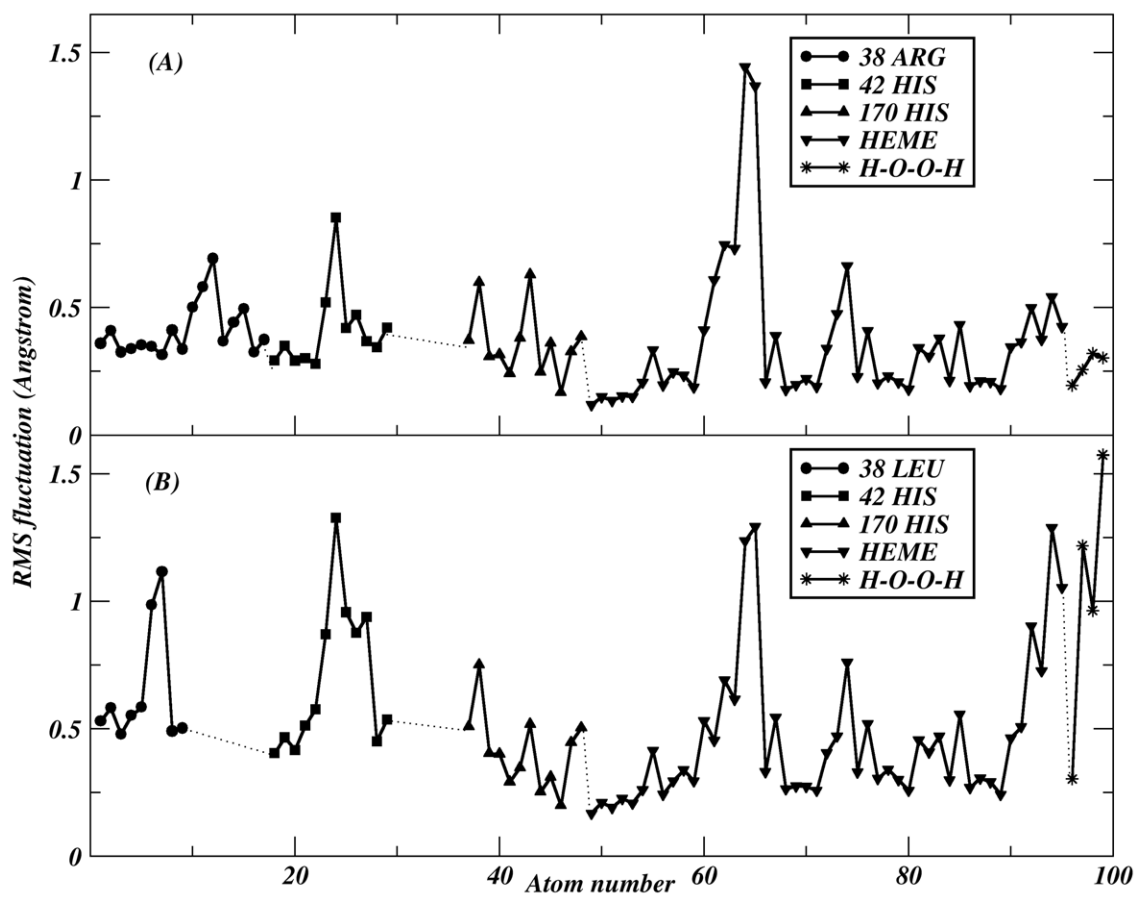
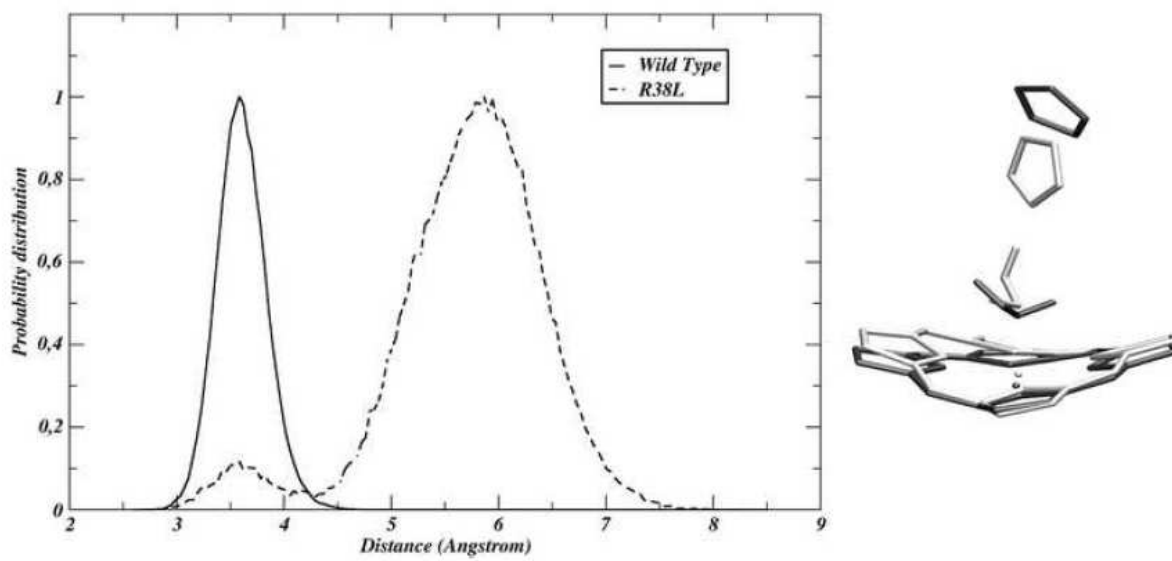




Fig 7



ACCEPTTEL

Fig 8

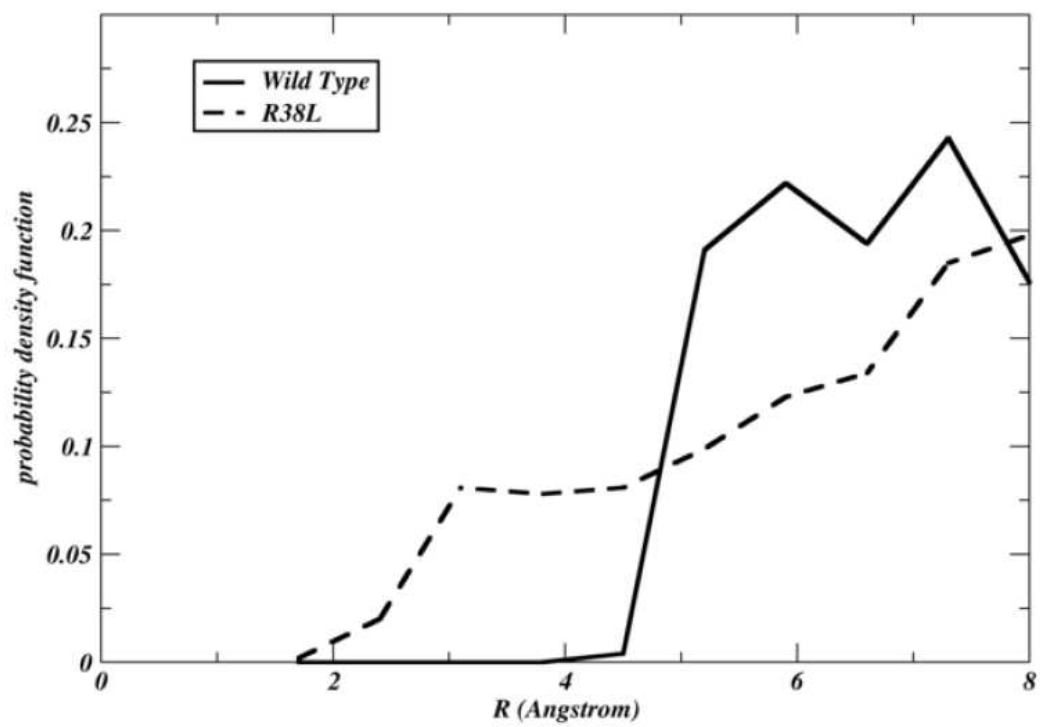
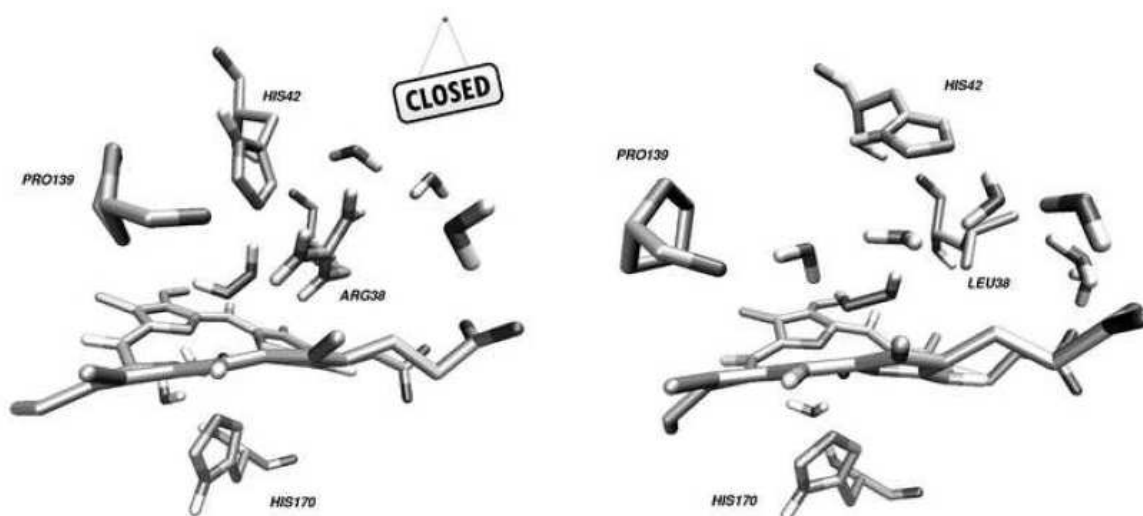


Fig 9



ACCEPTED

Fig 10

